Supplemental Material

Tracing human stem cell lineage during development using DNA methylation

Authors: Lucas A. Salas[1†], John K. Wiencke[2*†], Devin C. Koestler [3], Ze Zhang[4], Brock C. Christensen[1,5††], Karl T. Kelsey[4††].

Affiliations:
[1]Department of Epidemiology, Geisel School of Medicine, Dartmouth College, Lebanon NH.
[2]Department of Neurological Surgery, Institute for Human Genetics, University of California San Francisco, San Francisco CA.
[3]Department of Biostatistics, University of Kansas Medical Center, Kansas City KS.
[4]Departments of Epidemiology and Pathology and Laboratory Medicine, Brown University, Providence RI.
[5]Departments of Molecular and Systems Biology, and Community and Family Medicine, Geisel School of Medicine, Dartmouth College, Lebanon NH.
[*]Correspondence: John.Wiencke@ucsf.edu .
[†] Contributed equally
[††] Contributed equally

Table of contents

1. Discovery datasets

Cell-specific methylation data from Bcells, CD4T cells, CD8T cells, NK cells, Granulocytes, and Monocytes

Umbilical Cord-Blood (UCB)
(26 subjects, 151 samples)
Bakulski et al. (2016)
Gervin et al. (2016)

Adult Whole Blood (AWB)
(6 subjects, 36 samples)
Reinius et al. (2012)

2. Identify library of fetal cell origin markers

The following 3-step filtering process was employed

a) Across the six cell types, compare DNA methylation between UCB and AWB samples.
1,255 CpGs were identified as differentially methylated (Q<0.05) in all six cell types.

b) Filter to CpGs with consistent directional difference in methylation across all cell types where |Δβ| ≥ 0.1
1218 CpGs

c) Filter to CpGs with minimal residual cell-specific effects using principal components analysis.
27 CpGs

3. Estimate proportion of cells exhibiting the FCO signature

Using the final library of **27 CpGs**, **M**, our estimate of the fraction of cells carrying the FCO signature, **w**, for a given sample, **Y**, was based on the constrained projection quadratic programming (CP/QP) approach of Houseman et al. (2012). Specifically:

$$\arg\min_{\mathbf{w}} \| \mathbf{Y} - \mathbf{w}\mathbf{M}^T \|^2$$

4. Replication and Statistical Validation

Three orthogonal approaches were used to assess the reliability and validity of our FCO signature.

Replication using DNA methylation data on purified leukocyte cell types
GSE68456 (12 newborns, 45 samples)
GSE30870 (1 newborn and 1 adult sample)
GSE59065 (100 subjects, 199 samples)

Classification (AUROC) UCB and AWB DNA methylation profiles
GSE80310, GSE74738, GSE54399,
GSE79056, GSE62924 (123 newborns)
GSE74738, GSE54399 (34 adult subjects)

Synthetic cell mixtures with varying proportions of UCB and AWB DNA methylation profiles
GSE66459 (22 newborns)
GSE43976 (52 adult subjects)

Supplemental Fig. S1. Pipeline for discovery of Fetal Cell Origin (FCO) methylation signature

Supplemental Table S1. Data sources and citations

Discovery and validation datasets		Lymphocytes				Myeloid cells		Subjects			
	Repository	Bcell CD19+	CD4T CD4+	CD8T CD8+	NK CD56+	Gran Ficoll recovery	Mono CD14+	Females	Males	Total	Age mean(SD)
Discovery datasets											
Umbilical cord blood	FlowSorted.CordBlood.450K (Bakulski et al. 2016)	15	15	14	14	12	15	7	8	15	39.9(1.0) weeks
	FlowSorted.CordBloodNorway.450K (Gervin et al. 2016)	11	11	11	11	11	11	6	5	11	39.3(1.2) weeks
Peripheral blood	GSE35069 (Reinius et al. 2012)	6	6	6	6	6	6	0	6	6	38 (13.6) years
Replication datasets											
Umbilical cord blood	GSE68456 (de Goede et al. 2015)	7	7	6	6	7	12	7	5	12	Term newborns
	GSE30870 (Heyn et al. 2012)	0	1	0	0	0	0	NA	NA	1	Term newborn
Peripheral blood	GSE59065 (Tserel et al. 2015)	0	99	100	0	0	0	52	48	100	52.6(23.7) years
	GSE30870 (Heyn et al. 2012)	0	1	0	0	0	0	NA	NA	1	103 years

AUROC datasets	Repository	Whole blood	Females	Males	Total	Age mean(SD)
Umbilical cord blood	GSE80310 (Knight et al. 2016)	24	13	11	24	Term (38.1-42.9 weeks) newborns
	GSE74738 (Hanna et al. 2016)	1	0	0	1	Pooled sample (Unknown gestational age)
	GSE54399 (Montoya-Williams et al. 2017)	24	10	14	24	Term newborns, with unknown health conditions rural war area
	GSE79056 (Knight et al. 2016)	36	19	17	36	14 preterm (24.1-34 weeks), 22 term (39-40.9 weeks) newborns
	GSE62924 (Rojas et al. 2015)	38	22	16	38	39 (1.4) weeks
Peripheral blood	GSE74738 (Hanna et al. 2016)	10	10	0	10	29.0 (9.7) years (healthy women)
	GSE54399 (Montoya-Williams et al. 2017)	24	24	0	24	32.8 (7.4) years (unknown health conditions rural war area)

Synthetic mixtures datasets	Repository	Whole blood	Females	Males	Total	Age mean(SD)
Umbilical cord blood	GSE66459 (Fernando et al. 2015)	22	11	11	22	11 Term (38-41 weeks) and 11 preterm newborns (26-36 weeks)
Peripheral blood	GSE43976 (Marabita et al. 2013)	52	52	0	52	42.2(8.4) years (healthy women)

Embryonic stem cells, induced Pluripotent stem cells and hematopoietic cell progenitors**

Repository	ESC	iPSC	CD34+ fetal	Erythroid fetal	CD34+ Adult	MPP	L-MPP	CMP	GMP	MEP	Erythroid adult	PMC	PMN	Females	Males	Total	Age
GSE31848 (Nazor et al. 2012)	19	29	0	0	0	0	0	0	0	0	0	0	0	42	12	54	NA
GSE40799 (Weidner et al. 2013)	0	0	3	0	0	0	0	0	0	0	0	0	0	NA	NA	3	Term newborns
GSE56491 (Lessard et al. 2015)	0	0	0	12	0	0	0	0	0	0	0	0	0	NA	NA	12	Abortuses
GSE56491 (Lessard et al. 2015)	0	0	0	0	0	0	0	0	0	0	12	0	0	NA	NA	12	Adult bone marrow
GSE50797 (Rönnerblad et al. 2014)	0	0	0	0	0	0	0	3	3	0		3	3	1*	2*	3*	Adult bone marrow
GSE63409 (Jung et al. 2015)	**0**	**0**	**0**	**0**	**5**	**5**	**5**	**5**	**5**	**5**	**0**	**0**	**0**	2*	3*	5*	22-43 years

Somatic tissues											Subjects			
	Repository	Adrenal	Brain	Heart	Liver	Lung	Muscle	Pancreas	Spleen	Stomach	Females	Males	Total	Age
Fetal	GSE61279 (Bonder et al. 2014)	0	0	0	14	0	0	0	0	0	NA	NA	14	8-21 weeks
	GSE31848 (Nazor et al. 2012)	3	4	4	4	5	0	0	3	5	4*	2*	6*	14, 15, 18, and 20 weeks
	GSE56515 (Slieker et al. 2015)	9	0	0	0	0	9	8	0	0	NA	NA	10*	9,18 and 22 weeks
	GSE58885 (Spiers et al. 2015)	0	179	0	0	0	0	0	0	0	79	100	179	3-26 weeks
Adult	GSE61279 (Bonder et al. 2014)	0	0	0	96	0	0	0	0	0	48	48	96	26.8 (10.5) years
	GSE31848 (Nazor et al. 2012)	2	1	1	0	2	2	2	2	1	2*	1*	3*	48.0 (8.5) years
	GSE48472 (Slieker et al. 2013)	0	0	0	5	0	6	4	3	0	NA	NA	6*	52.5 (7.5) years
	GSE41826 (Guintivano et al. 2013)	0	29	0	0	0	0	0	0	0	15	14	29	33.3 (17.2) years

Aging datasets	Permanent repository	Whole blood	Mononuclear cells	Females	Males	Total	Age
Umbilical cord blood	FlowSorted.CordBlood.450K (Bakulski et al. 2016)	15	0	8	7	15	38.9 (1.3) weeks
	FlowSorted.CordBloodNorway.450K (Gervin et al. 2016)	11	0	6	5	11	39.3 (1.2) weeks
	GSE30870 (Heyn et al. 2012)	0	19	NA	NA	19	38.7 (1.9) weeks
	GSE83334 (Urdinguio et al. 2016)	15	0	9	6	15	38.9 (1.4) weeks

Aging datasets	Permanent repository	Whole blood	Mononuclear cells	Females	Males	Total	Age
Peripheral blood	GSE62219 (Acevedo et al. 2015)	60	0	60	0	60	2.3 (1.7) years
	GSE36054 (Alisch et al. 2012)	134	0	55	79	134	4.6 (4.1) years
	GSE40279 (Hannum et al. 2013)	656	0	338	318	656	64.0 (14.7) years
	GSE35069 (Reinius et al. 2012)	6	6	0	6*	6*	38 (13.6) years
	GSE30870 (Heyn et al. 2012)	0	19	NA	NA	19	92.6 (3.7) years
	GSE59065 (Tserel et al. 2015)	97	0	49	48	97	52.7 (23.7) years
	GSE83334 (Urdinguio et al. 2016)	15	0	9	6	15	5 years

*Several samples were drawn from the same subject

** ESC: undifferentiated embryonic stem cells, iPSC: undifferentiated induced pluripotent stem cells, $CD34^+$ fetal: stem/progenitor cells from fresh umbilical cord blood, erythroid fetal and adult: $CD34^+$ cells from fetal liver and bone marrow respectively differentiated *ex-vivo* to erythroid cells (transferrin receptor-$CD71^+$, and glycophorin-$CD235\alpha^+$), $CD34^+$ adult: $CD34^+CD38^-CD90^+CD45RA^-$, adult bone marrow progenitors samples: MPP-multipotent progenitors $CD34^+CD38^-CD90^-CD45RA^-$, L-MPP- lymphoid primed multipotent progenitors $CD34^+CD38^-CD90^-CD45RA^+$, CMP- common myeloid progenitors $CD34^+CD38^+CD123^+CD45RA^-$, GMP-granulocyte/macrophage progenitors $CD34^+CD38^+CD123^-CD45RA^+$, MEP-megakaryocyte-erythroid progenitors $CD34^+CD38^+CD123^-CD45RA^-$, $CD34^+$ myeloid progenitors: CMP- common myeloid progenitors $CD34^+CD38^+CD123^+CD110^-CD45RA^-$, and GMP-granulocyte/macrophage progenitors $CD34^+CD38^+CD123^+CD110^-CD45RA^+$, $CD34^-$ immature myeloid progenitors: PMC-promyelocyte/myelocyte $CD34^-$ $CD117^+CD33^+CD13^+CD11b^+$, PMN - metamyelocyte/band-myelocyte $CD34^-CD117^-CD33^+CD13^+CD11b^+$.

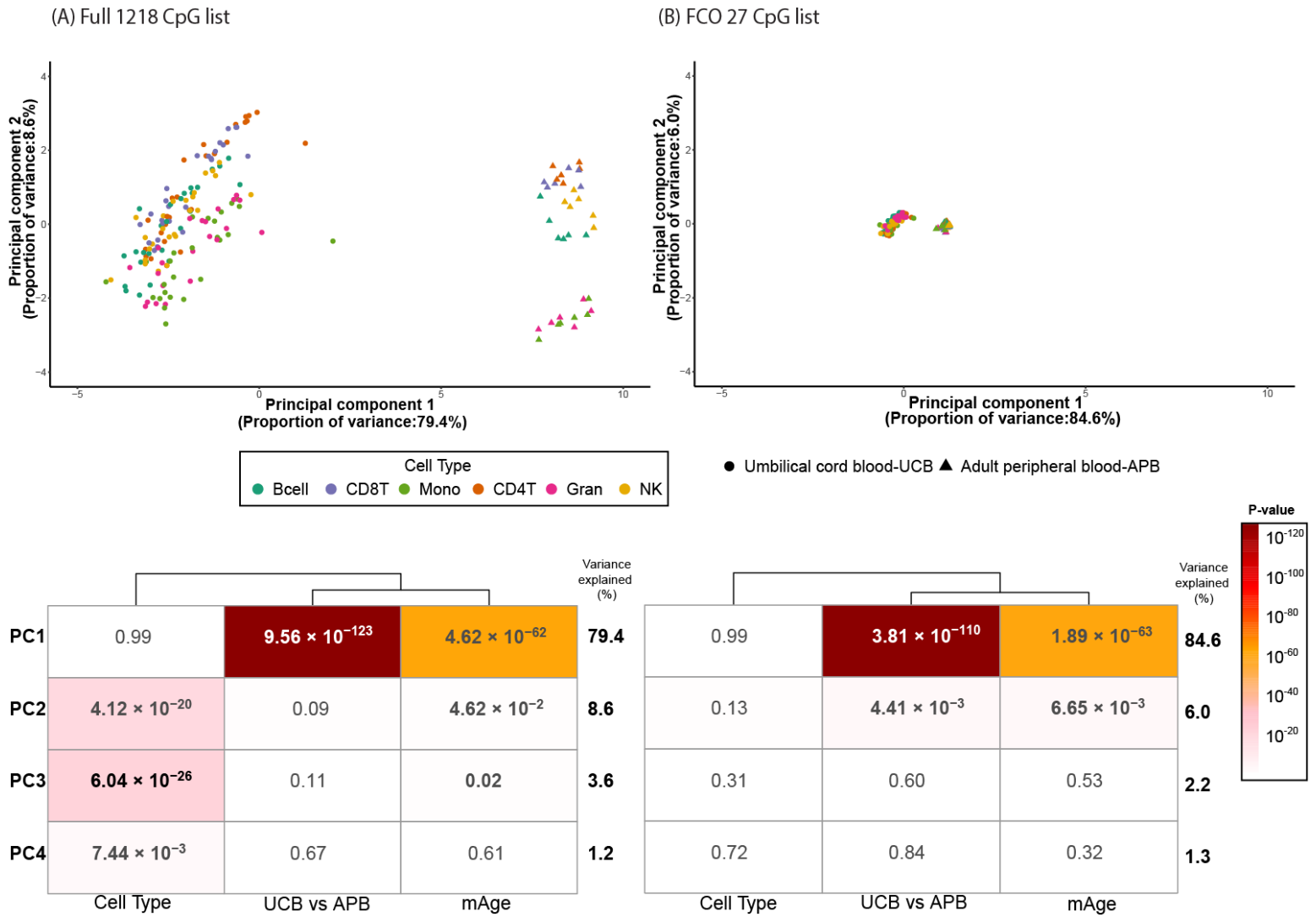

Supplemental Fig. S2. Selection of invariant loci for the fetal cell origin-FCO signature.
Panel A. Candidate loci (1,218 CpG) showed a high variability between umbilical cord blood and adult peripheral blood purified cells (principal component 1, x axis). Albeit small relative to the UCB/APB effect, there was a statistically significant cell type effect present among these 1,218 CpGs (principal components-PC 2 and 3, y axis upper panel and *P* heatmap in the lower panel in bold the significant variables). Panel B, the reduced library (27 CpGs), showed strong separation of UCB and APB samples (principal component 1, x axis), however the residual variability from cell type was attenuated (principal component 2, y axis upper panel, *P* heatmap lower panel). Abbreviations: mAge: DNA methylation age (Horvarth)

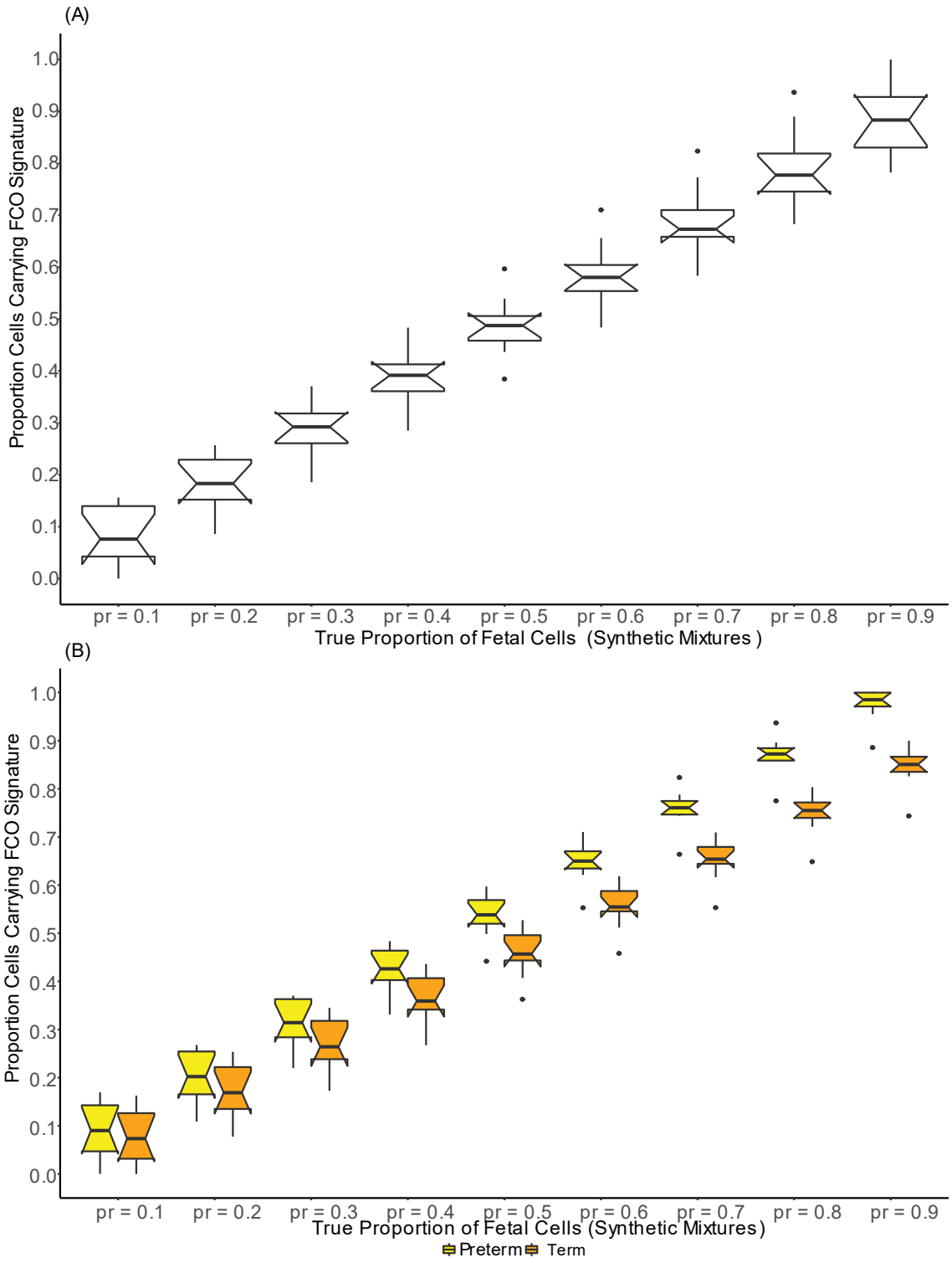

Supplemental Fig. S3. Synthetic Mixture experiment.
Panel A. When generating artificial synthetic mixtures, a high agreement was observed with a concordance correlation coefficient, CCC=0.97 (P<0.05). Panel B as we had samples from umbilical cord blood of preterms (<37 weeks of gestational age) and term newborns (≥37 weeks of gestation), we generated mixtures using these two different subgroups. The CCC for the mixtures using Preterm samples was slightly higher CCC=0.97 vs Term newborns CCC=0.96. Although there were differences with the largest proportions of cord blood mixtures, overall there were no statistically significant differences.

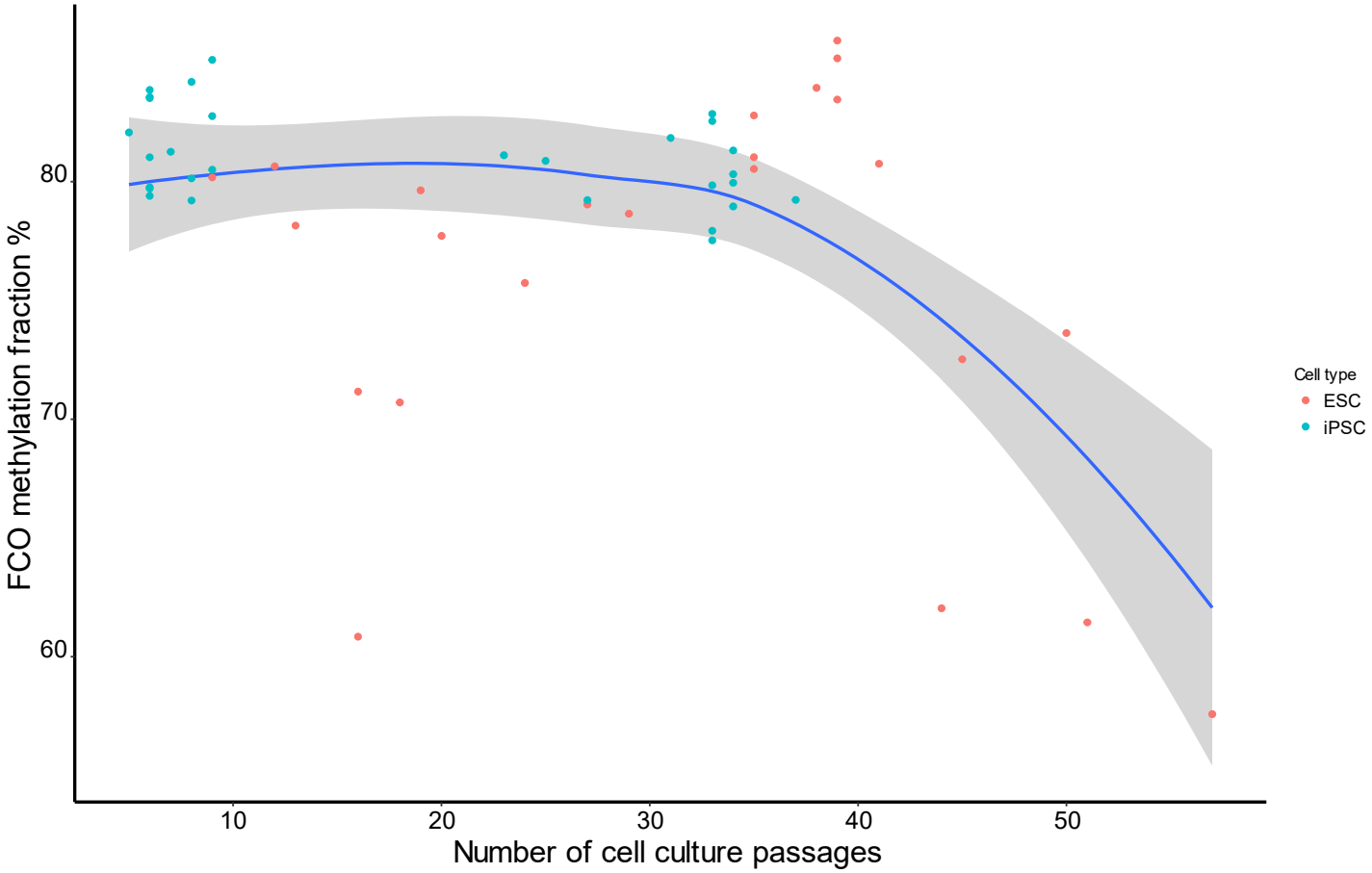

Supplemental Fig. S4. Estimated Fetal Cell Origin (FCO) in embryonic stem cells (ESC) and induced pluripotent stem cells (iPSC) through different number of cell culture passages (cell subcultures) using loess smoothing.

Notes: For the graph one observation with 105 passages was excluded. Number of passages ranging from 5 to 57 passages

Supplemental Table S2. Fetal Cell Origin (FCO) signature deconvolution in pluripotent, fetal progenitors and adult CD34$^+$ stem/progenitor cells.

Fetal/embryonic	Cell Type	n	mean (SD)
Fetal/embryonic	ESC	25	75.1 (9)
	iPSC	29	81 (1.9)
	CD34+ fetal	3	81.8 (2.3)
	Erythroid fetal	12	63.6 (3.3)
Adult progenitors (bone marrow)	CD34+ adult	5	12.1 (6.7)
	MPP	5	2.6 (3.8)
	L-MPP	5	4.3 (4.5)
	CMP	8	4.4 (3.7)
	GMP	8	4.8 (6.4)
	MEP	5	4.2 (4.5)
	Erythroid adult	12	2.8 (3.8)
	PMC	3	2.7 (4.7)
	PMN	3	2.1 (3.7)

Estimated mean (SD) FCO methylation fractions for embryonic/fetal cells are 75.9% (8.5) and 4.4% (5.1) for adult progenitors (bone marrow), $P = 1.81 \times 10^{-86}$.

Abbreviations: Embryonic stem cells (ESC), Induced Pluripotent Stem cells (iPSC), CD34$^+$ fetal (fresh cord blood cells expressing CD34$^+$), Erythroid fetal (fetal liver CD34$^+$ cells, differentiated *ex vivo* to express transferrin receptor and glycophorin), CD34$^+$ adult (bone marrow expressing CD34$^+$ CD38$^-$ CD90$^+$ CD45RA$^-$), Multipotent progenitors (MPP), Lymphoid primed multipotent progenitors (L-MPP), Common myeloid progenitors (CMP), Granulocyte/macrophage progenitors (GMP), Megakaryocyte-erythroid progenitors (MEP), Erythroid adult (adult bone marrow CD34$^+$ cells, differentiated ex vivo to express transferrin receptor and glycophorin), Promyelocyte/myelocyte (PMC), metamyelocyte/band-myelocyte (PMN).

Supplemental Table S3. MSigDB pathways test for enrichment with DMRs contained in lineage invariant developmentally sensitive loci (N= 1218).

						ToppGene			GREAT		missMethyl	
ID	**MSigDB Pathways**	**Cell target of the pathway**	**K**	**DM**	**DM (cis)**	***P***	**FDR**	**FE**	**P**	**FDR**	**P**	**FDR**
	Genes identified by ChIP on chip as targets of a Polycomb protein or Polycomb Repression Complex 2 (bound to protein and H3K27 tri-methylation (H3K27me3))											
M9898	BENPORATH_SUZ12_TARGETS	Human embryonic stem cells	1038	112	183	2.86×10^{-41}	1.33×10^{-37}	2.09	1.92×10^{-38}	1.61×10^{-35}	$<2.0 \times 10^{-16}$	$<2.0 \times 10^{-16}$
M7617	BENPORATH_EED_TARGETS	Human embryonic stem cells	1062	105	184	6.79×10^{-36}	1.58×10^{-32}	2.06	2.68×10^{-37}	1.80×10^{-34}	$<2.0 \times 10^{-16}$	$<2.0 \times 10^{-16}$
M8448	BENPORATH_PRC2_TARGETS	Human embryonic stem cells	652	83	138	3.49×10^{-36}	1.08×10^{-32}	2.59	4.19×10^{-46}	4.69×10^{-43}	$<2.0 \times 10^{-16}$	$<2.0 \times 10^{-16}$
	Genes with high-CpG-density promoters (HCP) bearing the H3K27 tri-methylation (H3K27me3)											
M10371	BENPORATH_ES_WITH_H3K27ME3	Human embryonic stem cells	1118	122	210	1.48×10^{-46}	1.38×10^{-42}	2.18	4.47×10^{-50}	7.51×10^{-47}	$<2.0 \times 10^{-16}$	$<2.0 \times 10^{-16}$
M1938	MEISSNER_BRAIN_HCP_WITH_H3K27ME3	Brain	269	39	80	2.16×10^{-19}	3.36×10^{-16}	3.71	1.31×10^{-51}	4.40×10^{-48}	2.90×10^{-12}	2.74×10^{-9}
M1967	MIKKELSEN_IPS_WITH_HCP_H3K27ME3	MCV8.1 (induced pluripotent cells, iPS)	102	22	28	3.53×10^{-15}	4.11×10^{-12}	4.99	7.61×10^{-36}	4.27×10^{-33}	8.32×10^{-10}	6.55×10^{-7}
M2009	MIKKELSEN_NPC_HCP_WITH_H3K27ME3	Neural progenitor cells (NPC)	341	39	78	8.50×10^{-16}	1.13×10^{-12}	2.38	2.12×10^{-21}	1.02×10^{-18}	1.97×10^{-8}	1.17×10^{-5}
M1932	MEISSNER_NPC_HCP_WITH_H3K27ME3	Neural precursor cells (NPC)	79	12	22	4.13×10^{-7}	1.60×10^{-4}	3.50	8.53×10^{-15}	2.61×10^{-12}	3.07×10^{-5}	9.06×10^{-3}
M1954	MIKKELSEN_MCV6_HCP_WITH_H3K27ME3	MCV6 cells (embryonic fibroblasts trapped in a differentiated state)	435	43		5.14×10^{-12}	5.00×10^{-11}			N.S	1.96×10^{-7}	9.27×10^{-5}
M2019	MIKKELSEN_MEF_HCP_WITH_H3K27ME3	MEF cells (embryonic fibroblast)	590	48		6.86×10^{-10}	6.66×10^{-9}			N.S	2×10^{-6}	8.47×10^{-4}
	Genes with high-CpG-density promoters (HCP) that have no H3K27 tri-methylation (H3K27me3)											
M1936	MEISSNER_NPC_HCP_WITH_H3_UNMETHYLATED	Neural precursor cells (NPC)	536	44	65	1.65×10^{-12}	1.18×10^{-9}	2.06	1.69×10^{-14}	4.36×10^{-12}	3.4×10^{-8}	1.79×10^{-5}
	Genes with high-CpG-density promoters (HCP) bearing histone H3 dimethylation at K4 (H3K4me2) and trimethylation at K27 (H3K27me3)											
M1941	MEISSNER_BRAIN_HCP_WITH_H3K4ME3_AND_H3K27ME3	Brain	1069	83		5.42×10^{-18}	5.26×10^{-17}			N.S	1.86×10^{-8}	1.17×10^{-5}
M1949	MEISSNER_NPC_HCP_WITH_H3K4ME2_AND_H3K27ME3	Neural precursor cells (NPC)	349	34		3.85×10^{-9}	3.74×10^{-8}			N.S	9.3×10^{-6}	3.38×10^{-3}
	Genes hypermethylated in tumor cells											
M19508	HATADA_METHYLATED_IN_LUNG_CANCER_UP	Lung cancer cells	390	32		4.05×10^{-6}	3.93×10^{-5}			N.S	2.5×10^{-5}	7.97×10^{-3}
	Genes up-regulated in tumor cells											
M2098	MARTENS_TRETINOIN_RESPONSE_UP	NB4 cells (acute promyelocytic leukemia, APL)	857	50		1.17×10^{-5}	1.14×10^{-4}			N.S	3.5×10^{-6}	1.36×10^{-3}

Note: the table summarizes only the significant pathways overlapping three different methods to test for enrichment: 1) ToppGene, hypergeometric distribution to test for enrichment, 2) GREAT, binomial test to test for enrichment cis-regulatory regions, and 3) missMethyl which allows adjusting for array bias.
Abbreviations: ID (MSigDB internal identifier), K (number of genes contained in the gene set), DM (differentially methylated genes overlapping the CpG site), DM (cis) (cis-regulatory regions either overlapping the differentially methylated CpG site or 1 Mb around the site), *P* (unadjusted *P*-value), FDR (False discovery), FE (Fold enrichment), N.S (not significant association, FDR>0.05)

Supplemental Table S4. Functional annotation using ENCODE data of the loci included in the FCO methylation signature

Probe ID	Human Embryonic Stem cell	Human umbilical vein endothelial cell	Transcription factor 1	Transcription factor 2
cg10338787	3_Poised_Promoter	12_Repressed	EZH2	EZH2
cg22497969	13_Heterochromatin/low signal	13_Heterochromatin/low signal		
cg11968804	3_Poised_Promoter	12_Repressed		
cg10237252	6_Weak_Enhancer	12_Repressed	Pol2	
cg17310258	3_Poised_Promoter	12_Repressed	EZH2	EZH2
cg13485366	13_Heterochromatin/low signal	13_Heterochromatin/low signal		
cg03455765	2_Weak_Promoter	12_Repressed		
cg04193160	3_Poised_Promoter	12_Repressed	USF-1	Bach1
cg27367526	2_Weak_Promoter	1_Active_Promoter		
cg03384000	3_Poised_Promoter	1_Active_Promoter	SIN3A	
cg15575683	3_Poised_Promoter	12_Repressed	YY1	
cg17471939	3_Poised_Promoter	13_Heterochromatin/low signal		
cg11199014	3_Poised_Promoter	3_Poised_Promoter	Pol2	RBBP5
cg13948430	3_Poised_Promoter	12_Repressed		
cg01567783	3_Poised_Promoter	12_Repressed		
cg01278041	2_Weak_Promoter	11_Weak_Transcribed	CHD1	TAF1
cg19005955	7_Weak_Enhancer	4_Strong_Enhancer		
cg16154155	3_Poised_Promoter	12_Repressed	EZH2	EZH2
cg14652587	3_Poised_Promoter	12_Repressed		
cg19659741	6_Weak_Enhancer	12_Repressed		
cg06705930	3_Poised_Promoter	12_Repressed	SUZ12	
cg23009780	5_Strong_Enhancer	12_Repressed		
cg22130008	3_Poised_Promoter	3_Poised_Promoter		
cg05840541	13_Heterochromatin/low signal	13_Heterochromatin/low signal		
cg06953130	2_Weak_Promoter	5_Strong_Enhancer		
cg11194994	2_Weak_Promoter	4_Strong_Enhancer		
cg14375747	6_Weak_Enhancer	12_Repressed	TBP	

Supplemental Table S5. Transcription factors with DMRs contained in lineage invariant developmentally sensitive loci (N= 1218).

Transcription factor	Name
Zinc-coordinating DNA-binding domains	
KLF9	Kruppel Like Factor 9
ZBTB46	Zinc Finger BTB Domain Containing 46
PRDM10	PR/SET Domain 10
PRDM16	PR/SET Domain 12
Helix-turn-helix domains	
Homeo domain factors	
HOXA2	Homeobox A2
HOXB7	Homeobox B7
HOXB-AS3	HOXB Cluster Antisense RNA 3
LBX2	Ladybird Homeobox 2
VAX2	Ventral Anterior Homeobox 2
ALX4	ALX Homeobox 4
PITX3	Paired Like Homeodomain 3
LHX6	LIM Homeobox 6
SIX2	SIX homeobox 2
POU2F1 (Oct-1)	POU Class 2 Factor 1
POU3F1 (Oct-6)	POU Class 3 Homeobox 1
Paired box factors	
PAX6	Homeodomain Paired box 6
PAX8	Homeodomain Paired box 8
FOXE3	Forkhead binding E3
FOXD2	Forkhead binding D2
FOXI2	Forkhead binding I2
FOXL2	Forkhead binding L2
FOXL2NB	FOXL2 Neighbor
Tryptophan cluster factors	
ETV4	ETS variant 4
ARID	
ARID3A	AT-Rich Interaction Domain 3A
Other all-α-helical DNA-binding domains	
SOX18	SRY-Box 18
Immunoglobulin fold	
TBX1	T-Box 1
TBX4	T-Box 4
β-Hairpin exposed by an α/β-scaffold	
NF-1X	Nuclear Factor 1 X

Supplemental Table S6. Progenitor Cell Biology Consortium (PCBC) pathways test for enrichment using ToppGene with DMRs contained in lineage invariant developmentally sensitive loci (N= 1218).

PCBC Pathway	# Genes in Gene Set (K)	DM	*P*	FDR
Stem cells top expressed genes				
Arv_EB-LF_2500_K2	960	59	3.21×10^{-10}	1.04×10^{-8}
Arv_EB-LF_1000	990	58	2.73×10^{-9}	7.62×10^{-8}
Arv_EB-LF_1000_K4	436	33	2.67×10^{-8}	5.66×10^{-7}
Arv_EB-LF_500_K2	256	23	1.77×10^{-7}	3.11×10^{-6}
PCBC_SC_CD34+_1000	987	53	2.33×10^{-7}	3.77×10^{-6}
Arv_EB-LF_500	499	32	1.75×10^{-6}	2.45×10^{-5}
Arv_SC-LF_1000_K3	679	39	2.01×10^{-6}	2.74×10^{-5}
Embryoid body vs Stem Cells				
PCBC_ratio_EB_vs_SC_1000	997	86	8.85×10^{-24}	5.43×10^{-21}
ratio_EB_vs_SC_2500_K3	1102	79	4.62×10^{-17}	9.46×10^{-15}
PCBC_ratio_EB_vs_SC_500	499	47	1.01×10^{-14}	1.03×10^{-12}
ratio_EB_vs_SC_1000_K5	418	42	3.14×10^{-14}	2.75×10^{-12}
ratio_EB_vs_SC_1000_K1	336	29	1.09×10^{-8}	2.67×10^{-7}
ratio_EB_vs_SC_500_K3	204	22	1.26×10^{-8}	2.98×10^{-7}
Ectoderm vs Stem cell				
ratio_ECTO_vs_SC_2500_K3	854	60	9.51×10^{-13}	5.84×10^{-11}
ratio_ECTO_vs_SC_500_K1	283	32	1.67×10^{-12}	9.34×10^{-11}
ratio_ECTO_vs_SC_1000_K3	476	42	2.47×10^{-12}	1.26×10^{-10}
PCBC_ratio_ECTO_vs_SC_500	499	42	1.14×10^{-11}	5.01×10^{-10}
PCBC_ratio_ECTO_vs_SC_1000	994	61	1.65×10^{-10}	5.64×10^{-9}
PCBC_ratio_ECTO_vs_SC_100	100	14	2.32×10^{-7}	3.77×10^{-6}
Endoderm vs Stem cell				
PCBC_ratio_DE_vs_SC_500	499	36	2.13×10^{-8}	4.66×10^{-7}
ratio_DE_vs_SC_500_K5	300	26	5.79×10^{-8}	1.15×10^{-6}
ratio_DE_vs_SC_500_K1	377	29	1.34×10^{-7}	2.50×10^{-6}
ratio_DE_vs_SC_1000_K5	542	36	1.68×10^{-7}	3.03×10^{-6}
PCBC_ratio_DE_vs_SC_1000	998	49	8.25×10^{-6}	1.01×10^{-4}
ratio_DE_vs_SC_1000_K2	523	31	1.24×10^{-5}	1.43×10^{-4}
Mesoderm vs Stem cell				
PCBC_ratio_MESO-5_vs_SC_500	499	34	2.06×10^{-7}	3.51×10^{-6}
PCBC_ratio_MESO-5_vs_SC_1000	994	51	1.53×10^{-6}	2.24×10^{-5}
ratio_MESO_vs_SC_500_K1	297	22	8.01×10^{-6}	1.00×10^{-4}
Embryoid body top expressed genes				
PCBC_EB_1000	997	81	9.22×10^{-21}	2.83×10^{-18}
PCBC_EB_500	499	45	1.82×10^{-13}	1.40×10^{-11}
Embryoid body vs non-stem cells				
PCBC_EB_blastocyst_1000	995	74	7.21×10^{-17}	1.11×10^{-14}
PCBC_EB_fibroblast_1000	992	71	2.38×10^{-15}	2.93×10^{-13}
PCBC_EB_fibroblast_500	499	44	7.42×10^{-13}	5.06×10^{-11}

PCBC Pathway	# Genes in Gene Set (K)	DM	*P*	FDR
PCBC_EB_blastocyst_500	498	41	4.04×10^{-11}	1.55×10^{-9}
Ectoderm top expressed genes				
PCBC_ECTO_fibroblast_1000	996	62	6.46×10^{-11}	2.33×10^{-9}
PCBC_ECTO_fibroblast_500	499	39	5.61×10^{-10}	1.72×10^{-8}
PCBC_ECTO_500	498	37	6.18×10^{-9}	1.65×10^{-7}
PCBC_ECTO_1000	997	57	9.06×10^{-9}	2.32×10^{-7}
PCBC_ECTO_blastocyst_1000	986	56	1.55×10^{-8}	3.53×10^{-7}
PCBC_ECTO_blastocyst_500	490	34	1.34×10^{-7}	2.50×10^{-6}
Mesoderm top expressed genes				
PCBC_MESO-5_blastocyst_1000	979	52	4.26×10^{-7}	6.71×10^{-6}
PCBC_MESO-5_fibroblast_1000	985	50	2.64×10^{-6}	3.53×10^{-5}
PCBC_MESO-5_500	494	30	1.08×10^{-5}	1.29×10^{-4}
Other differentiated cells				
JC_fibro_1000	994	64	7.28×10^{-12}	3.44×10^{-10}
geo_heart_1000_K5	428	38	2.36×10^{-11}	9.67×10^{-10}
JC_fibro_500	497	38	1.74×10^{-9}	5.08×10^{-8}
PCBC_ctl_geo-heart_1000	997	55	5.60×10^{-8}	1.15×10^{-6}
JC_fibro_2500_K5	826	43	7.36×10^{-6}	9.42×10^{-5}
JC_fibro_1000_K4	177	16	1.22×10^{-5}	1.43×10^{-4}

Supplemental Table S7. Age specific estimated FCO methylation fractions in blood leukocytes from birth to old age

Age group	N	Min.	P10	P25	Median	Mean	SD	P75	P90	Max.	*P*
Newborn	60	67.5	74.4	78.5	82.3	82.0	6.0	85.6	88.8	97.6	Reference
<12mo	32	15.7	23.9	28.6	42.0	44.5	17.6	57.7	68.0	75.0	2.13×10^{-134}
12-18mo	17	22.7	25.5	29.1	30.4	31.8	5.0	36.4	38.0	39.4	2.13×10^{-134}
18-24mo	23	5.9	13.4	22.9	25.9	26.6	13.2	28.9	35.9	62.5	1.34×10^{-147}
2-5yr	106	0	2.5	9.1	15.2	14.7	8.3	20.8	24.2	37.0	5.95×10^{-198}
5-18yr	31	0	0	0	0.5	4.3	6.8	6.7	13.2	28.7	$<2.23 \times 10^{-308}$
18-65yr	403	0	0	0	0	3.1	4.5	5.6	9.43	26.5	$<2.23 \times 10^{-308}$
>65yr	381	0	0	0	0	1.6	3.5	1.5	5.97	25.8	$<2.23 \times 10^{-308}$

Notes: Minimum, maximum, percentile cutoff values (10, 25, 50, 75, 90), mean and standard deviations derived from population data combined from published methylation datasets: see Supplemental Table S1. Values < 0.1 were coded as 0. The reported *P* are based on linear model estimations adjusting for the age group using the newborns as the reference. We also used a linear mixed effect model adjusting for subject (for those measures with several samples), and Study as random effects, the *P* (using the Kenward Roger approximation for the degrees of freedom) were $<2.23 \times 10^{-308}$ for all the groups compared to the newborns.

Supplemental Methods S1. Stability of the FCO calculations

To establish the stability of the FCO signature, we evaluated the absolute difference in the FCO estimates when all the potential combinations of one to five CpGs were lost during the FCO estimations compared to the full set of 27 CpGs using the samples used for the AUROC analysis (umbilical cord blood GSE80310 (Knight et al. 2016), GSE74738 (Hanna et al. 2016), GSE54399 (Montoya-Williams et al. 2017), GSE79056 (Knight et al. 2016), GSE62924 (Rojas et al. 2015). Adult peripheral blood GSE74738 (Hanna et al. 2016), GSE54399 (Montoya-Williams et al. 2017). We also calculated the average root mean square error (RMSE) between the prediction using the 27 CpGs vs all the potential combinations when as few as one CpG and as many as five CpGs were excluded from the 27 FCO CpGs. Our results indicate that the 27 CpG sites is a minimum discriminatory set for a reliable FCO estimation.

Within the 27 CpGs the loss of eight probes (cg01278041, cg05840541, cg11194994, cg11199014, cg13485366, cg14652587, cg17471939, cg22497969) had the biggest impact in the FCO calculations (RMSE>10). In contrast the loss of some other probes (e.g. cg01567783, absent in the EPIC array), only altered minimally the FCO estimates (RMSE:2.24). We suggest that the full set of probes will be used for the calculations but in the absence of specific probes the researcher should consider the increase in the estimation errors.

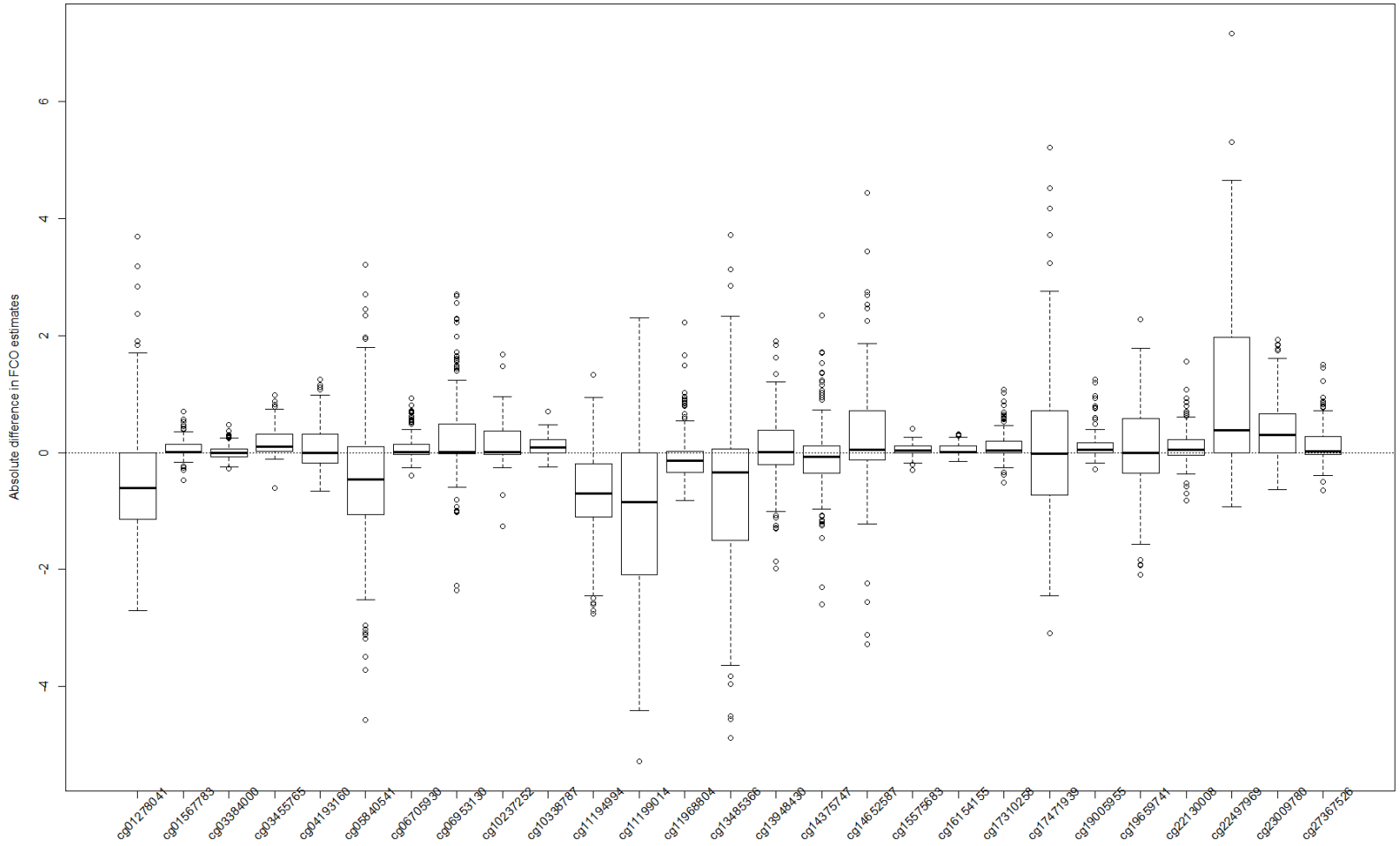

Supplemental Methods S1 Figure 1. Absolute difference between FCO estimated with one of the CpG probe lost versus the full set of 27 CpGs

Note: the y axis represent the difference in percentages

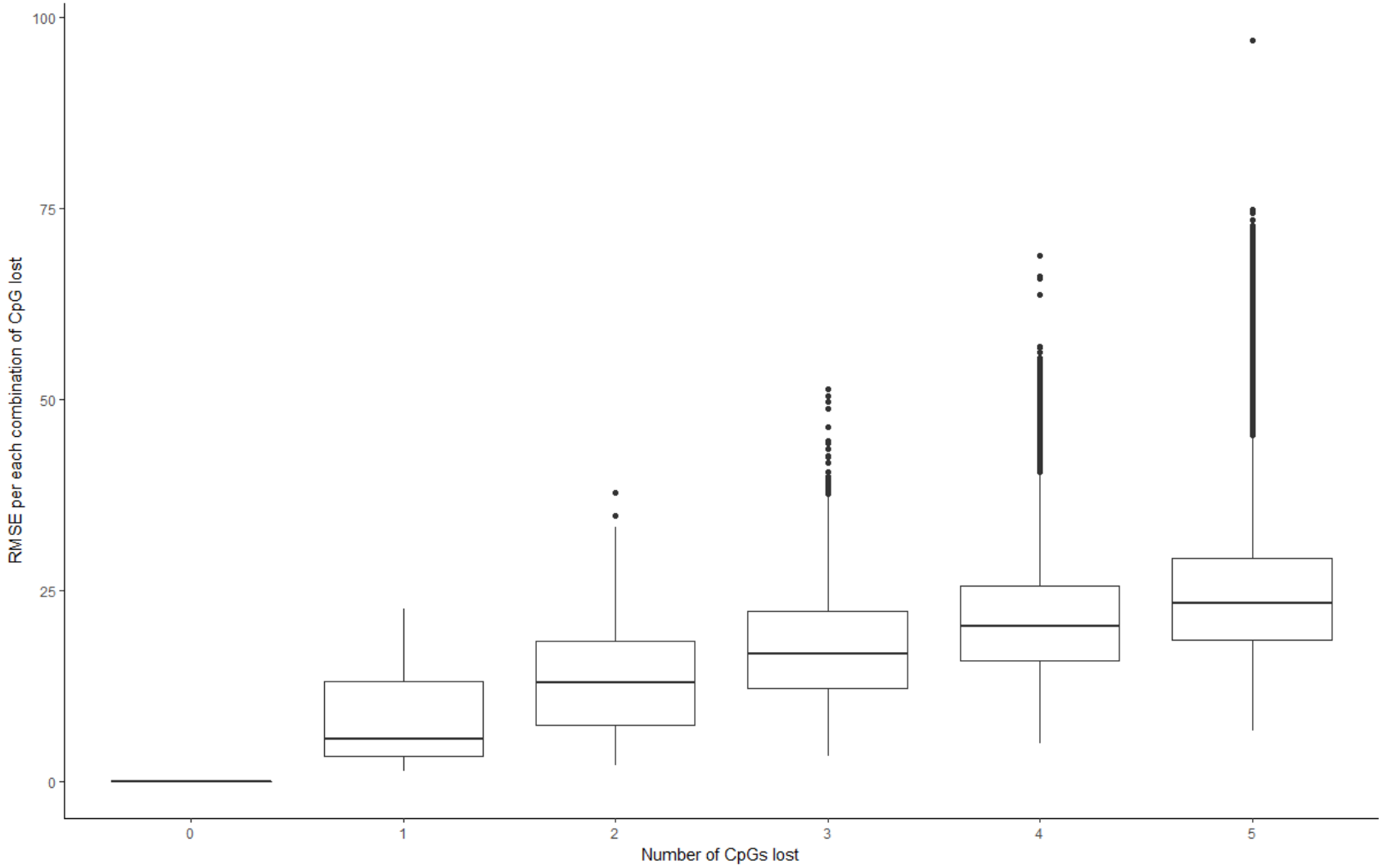

Supplemental Methods S1 Figure 2. Root Mean Square Error increase per CpG lost

Notes: In the x axis 0 corresponds to the reference including the 27 CpGs, 1, corresponds to 27 combinations losing one CpG, 2 to 351 combinations losing 2 CpGs, 3 to 2925 combinations losing 3 CpGs, 4 to 17550 combinations losing four CpGs, and 5 to 80730 combinations losing 5 CpGs.

Supplemental Methods S2. Synthetic mixture statistical validation

To establish the reliability of our fetal deconvolution methodology, we performed an additional experiment that involved first creating, and then deconvoluting synthetic mixtures of fetal UCB and adult peripheral blood DNA methylation profiles mixed in in predetermined proportions. To more precisely describe our approach, let $\boldsymbol{S}^{CB}$ and $\boldsymbol{S}^{A}$ represent $J \times 1$ vectors of methylation β-values for fetal UCB and adult peripheral blood (Fernando et al. 2015; Marabita et al. 2013), respectively, with J denoting the number of CpG loci. The synthetic mixture, **M**, was generated as weighted linear combination of $\boldsymbol{S}^{CB}$ and $\boldsymbol{S}^{A}$, such that: $\mathbf{M} = \pi\, \boldsymbol{S}^{CB} + (1\text{-}\pi)\, \boldsymbol{S}^{A}$ and $0 \leq \pi \leq 1$. Assuming that $\boldsymbol{S}^{CB}$ and $\boldsymbol{S}^{A}$ represent the DNA methylation profile over "pure" populations of fetal and adult cells, respectively, π represents the fraction of cells carrying the FCO signature within the synthetic mixture, **M**. Application of cell mixture deconvolution to **M** using the FCO signature library allowed us to estimate the fraction of cells carrying the FCO signature, $\hat{\pi}$, which we compared to the "known" predetermined proportion, π.

To simulate synthetic mixtures we used two additional DNA methylation data sets: GSE66459 a fetal UCB (n = 22) data set (Fernando et al. 2015) and GSE43976 restricting to those samples of adult peripheral blood (n = 52) data set (Marabita et al. 2013). Importantly, neither of these data sets was used to identify or derive the FCO signature that forms the basis of deconvolution, and therefore represent truly independent data sets. Synthetic mixtures were generated by mixing randomly selected samples from both the fetal UCB and adult peripheral blood data sets, where the mixing parameter was selected to be $\pi = \{0.1, 0.2, 0.3, 0.4, 0.5, 0.6, 0.7, 0.8, 0.9\}$. For each specification of π, $n = 10$ synthetic mixture were generated.

Supplemental Methods S3. Maternal contamination sensitivity analyses

During the peer review of this manuscript, one of the reviewers raised our attention to a recently published manuscript describing a marker for maternal blood contamination in cord blood samples (Morin et al. 2017). We thank the reviewer for this important observation; it was very helpful and stimulated a great deal of thinking for the authors. Clearly maternal blood is a potential issue for contaminating cord blood in our setting and we appreciate the reviewer bringing this to our attention.

Those researchers developed a signature of blood maternal contamination using 10 probes from the 450K array and validated their results using three pyrosequenced CpGs. Morin et al. used the Reinius et al. dataset (Reinius et al. 2012) as an adult comparison and whole umbilical cord blood samples to detect differences in a linear model without further adjustment by age. They found 2,250 CpGs as potential targets for the differences between adult peripheral blood and cord blood based on mixed samples, rather than purified cells. They used a random forest approach to select a subset of highly hypomethylated 10 CpGs in the cord blood, none of these CpGs were present within our FCO signature. From this set of 10 CpGs, they developed a semi-quantitative index, wherein if more than 5 CpGs out of 10 demonstrated greater than a 20% difference in methylation, then that sample would qualify as being suspicious of maternal contamination. Although their filtering was based on a strict statistical rule, declaration of contamination mostly involved a qualitative assessment.

In response to the reviewer's concern, we assessed whether any potential maternal contamination had occurred in our datasets using the method from Morin et al. Only one donor sample

comprising all 6 isolated cells (indicated on the right side of the heatmap below) clustered slightly apart from the other samples (Supplemental Methods Figure 1). However, the DNA methylation age estimated for this sample (range: 0.82-2.95 years) was consistent with a UCB sample. We also clarified that the DNA methylation age margin of error reported by Horvath was >3.6 years (Horvath 2013). Thus, while the reviewer has raised a legitimate potential concern, we conclude there is no evidence of significant contamination in the discovery data set that we used. Nonetheless, we performed a sensitivity analysis eliminating all six cells from that sample and observed stable results. As the results were consistent, we only included the information of the sensitivity analyses in the Methods section and summarize this information for the reader here.

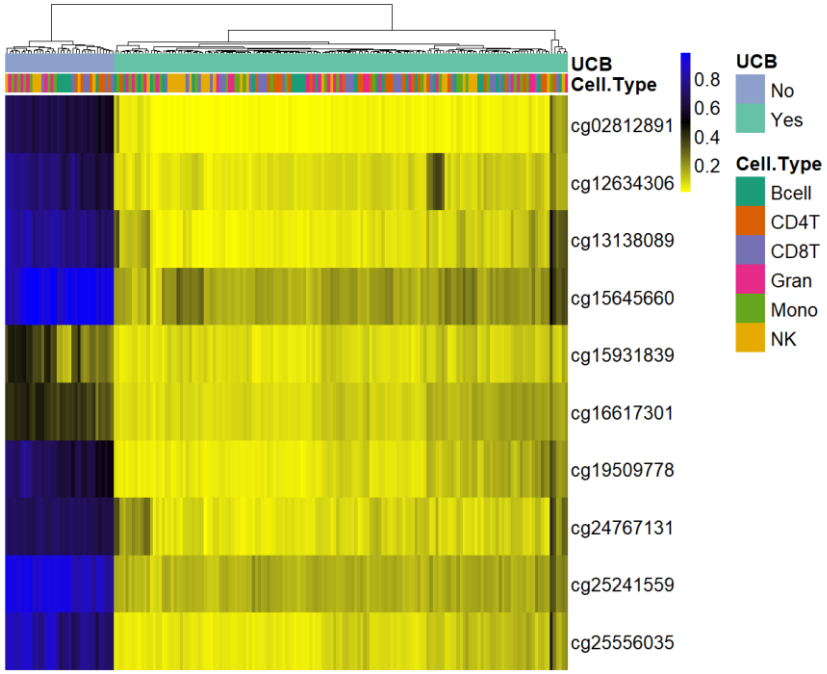

Supplemental Methods S3 Figure 1. Evaluation of potential maternal contamination in the discovery datasets
Notes: umbilical cord blood (UCB).

To further explore the idea of fetal contamination using the Morin makers we also explored our validation dataset and achieved the same results (Supplemental Methods Figure 2).

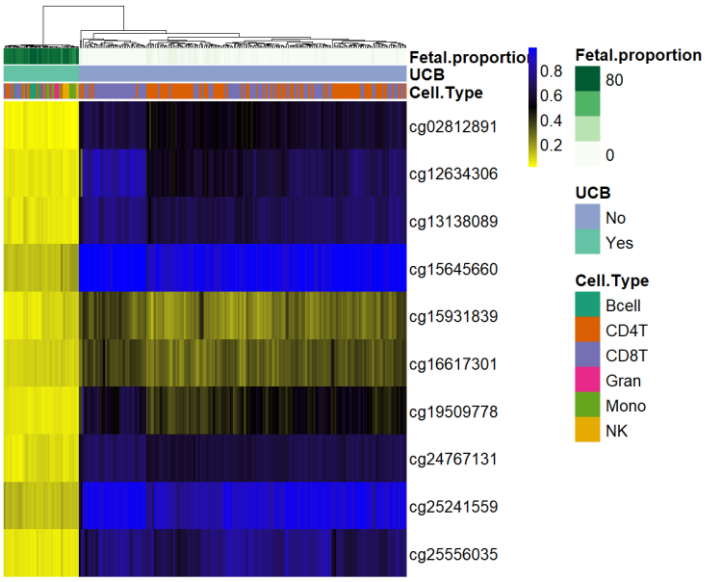

Supplemental Methods S3 Figure 2. Evaluation of potential maternal contamination in the validation datasets
Notes: umbilical cord blood (UCB), FCO estimated proportion (Fetal.proportion).

None of the samples were marked as suspicious using the Morin criteria.

Therefore, we do not believe the evidence supports maternal contamination as a factor influencing the validity or interpretation of our cord blood samples or any of the other fetal and adult data.

Morin et al. used five additional datasets that were not included in our first submission of the manuscript and they were included after the peer review. Using the 10 CpGs in Morin et al. we observed that one sample among the new data is clearly contaminated with maternal blood (Supplemental Methods Figure 3). The contaminated sample clusters with adult blood and has

FCO signature of 0%, as observed in the heatmap below. In addition, when calculating the DNA methylation age of this sample we estimated 44.5 years in the "cord blood sample" vs 45 years in the maternal blood pair. As not all Morin et al. CpGs were present in the GEO datasets accessed, we used a K-nearest neighbors imputation to predict the 10 CpGs in cases where data were missing. As this additional dataset (GSE54399) was used in the final manuscript we excluded this sample from the analyses. Taken together, these exercises give us confidence that we are able to detect maternal contamination using a combination of the Morin et al approach and the estimation of the DNA methylation age, should it exist, and that we can rule this factor out as playing a significant role in our final results.

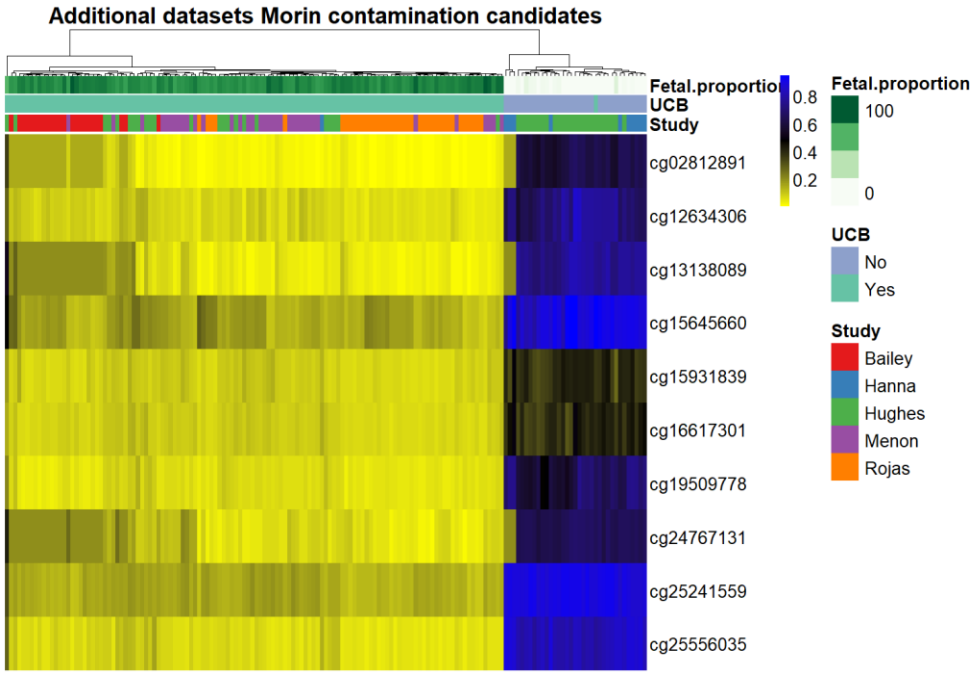

Supplemental Methods S3 Figure 3. Evaluation of potential maternal contamination in the five independent datasets compared to the FCO estimation
Notes: umbilical cord blood (UCB), FCO estimated proportion (Fetal.proportion).

Supplemental File S1. List of 1218 candidate loci detected and the selected candidates (see Excel file)

Supplemental Material References

Acevedo N, Reinius LE, Vitezic M, Fortino V, Söderhäll C, Honkanen H, Veijola R, Simell O, Toppari J, Ilonen J, et al. 2015. Age-associated DNA methylation changes in immune genes, histone modifiers and chromatin remodeling factors within 5 years after birth in human blood leukocytes. *Clin Epigenetics* **7**: 34.

Alisch RS, Barwick BG, Chopra P, Myrick LK, Satten GA, Conneely KN, Warren ST. 2012. Age-associated DNA methylation in pediatric populations. *Genome Res* **22**: 623–632.

Bakulski KM, Feinberg JI, Andrews S V., Yang J, Brown S, L. McKenney S, Witter F, Walston J, Feinberg AP, Fallin MD. 2016. DNA methylation of cord blood cell types: Applications for mixed cell birth studies. *Epigenetics* **11**: 354–362.

Bonder MJ, Kasela S, Kals M, Tamm R, Lokk K, Barragan I, Buurman WA, Deelen P, Greve J, Ivanov M, et al. 2014. Genetic and epigenetic regulation of gene expression in fetal and adult human livers. *BMC Genomics* **15**: 860.

de Goede OM, Razzaghian HR, Price EM, Jones MJ, Kobor MS, Robinson WP, Lavoie PM. 2015. Nucleated red blood cells impact DNA methylation and expression analyses of cord blood hematopoietic cells. *Clin Epigenetics* **7**: 95.

Fernando F, Keijser R, Henneman P, van der Kevie-Kersemaekers A-MF, Mannens MM, van der Post JA, Afink GB, Ris-Stalpers C. 2015. The idiopathic preterm delivery methylation profile in umbilical cord blood DNA. *BMC Genomics* **16**: 736.

Gervin K, Page CM, Aass HCD, Jansen MA, Fjeldstad HE, Andreassen BK, Duijts L, van Meurs JB, van Zelm MC, Jaddoe VW, et al. 2016. Cell type specific DNA methylation in cord blood: a 450K-reference data set and cell count-based validation of estimated cell type composition. *Epigenetics* **2294**: 00–00.

Guintivano J, Aryee MJ, Kaminsky ZA. 2013. A cell epigenotype specific model for the correction of brain cellular heterogeneity bias and its application to age, brain region and major depression. *Epigenetics* **8**: 290–302.

Hanna CW, Peñaherrera MS, Saadeh H, Andrews S, McFadden DE, Kelsey G, Robinson WP. 2016. Pervasive polymorphic imprinted methylation in the human placenta. *Genome Res* **26**: 756–67.

Hannum G, Guinney J, Zhao L, Zhang L, Hughes G, Sadda S, Klotzle B, Bibikova M, Fan JB, Gao Y, et al. 2013. Genome-wide Methylation Profiles Reveal Quantitative Views of Human Aging Rates. *Mol Cell* **49**: 359–367.

Heyn H, Li N, Ferreira HHJ, Moran S, Pisano DG, Gomez A, Diez J. 2012. Distinct DNA methylomes of newborns and centenarians. *Proc Natl Acad Sci U S A* **109**: 10522–10527.

Horvath S. 2013. DNA methylation age of human tissues and cell types. *Genome Biol* **14**: R115.

Jung N, Dai B, Gentles AJ, Majeti R, Feinberg AP. 2015. An LSC epigenetic signature is largely mutation independent and implicates the HOXA cluster in AML pathogenesis. *Nat Commun* **6**: 8489.

Knight AK, Craig JM, Theda C, Bækvad-Hansen M, Bybjerg-Grauholm J, Hansen CS, Hollegaard M V, Hougaard DM, Mortensen PB, Weinsheimer SM, et al. 2016. An epigenetic clock for gestational age at birth based on blood methylation data. *Genome Biol* **17**: 206.

Lessard S, Beaudoin M, Benkirane K, Lettre G. 2015. Comparison of DNA methylation profiles in human fetal and adult red blood cell progenitors. *Genome Med* **7**: 1.

Marabita F, Almgren M, Lindholm ME, Ruhrmann S, Fagerström-Billai F, Jagodic M, Sundberg CJ, Ekström TJ, Teschendorff AE, Tegnér J, et al. 2013. An evaluation of analysis pipelines

for DNA methylation profiling using the Illumina HumanMethylation450 BeadChip platform. *Epigenetics* **8**: 333–46.

Montoya-Williams D, Quinlan J, Clukay C, Rodney NC, Kertes DA, Mulligan CJ. 2017. Associations between maternal prenatal stress, methylation changes in IGF1 and IGF2, and birth weight. *J Dev Orig Health Dis* **9**: 1–8.

Morin AM, Gatev E, McEwen LM, MacIsaac JL, Lin DTS, Koen N, Czamara D, Räikkönen K, Zar HJ, Koenen K, et al. 2017. Maternal blood contamination of collected cord blood can be identified using DNA methylation at three CpGs. *Clin Epigenetics* **9**: 75.

Nazor KL, Altun G, Lynch C, Tran H, Harness J V., Slavin I, Garitaonandia I, Müller FJ, Wang YC, Boscolo FS, et al. 2012. Recurrent variations in DNA methylation in human pluripotent stem cells and their differentiated derivatives. *Cell Stem Cell* **10**: 620–634.

Reinius LE, Acevedo N, Joerink M, Pershagen G, Dahlén SE, Greco D, Söderhäll C, Scheynius A, Kere J. 2012. Differential DNA methylation in purified human blood cells: Implications for cell lineage and studies on disease susceptibility. *PLoS One* **7**.

Rojas D, Rager JE, Smeester L, Bailey KA, Drobná Z, Rubio-Andrade M, Stýblo M, García-Vargas G, Fry RC. 2015. Prenatal arsenic exposure and the epigenome: identifying sites of 5-methylcytosine alterations that predict functional changes in gene expression in newborn cord blood and subsequent birth outcomes. *Toxicol Sci* **143**: 97–106.

Rönnerblad M, Andersson R, Olofsson T, Douagi I, Karimi M, Lehmann S, Hoof I, de Hoon M, Itoh M, Nagao-Sato S, et al. 2014. Analysis of the DNA methylome and transcriptome in granulopoiesis reveals timed changes and dynamic enhancer methylation. *Blood* **123**: e79-89.

Slieker RC, Bos SD, Goeman JJ, Bovée JV, Talens RP, van der Breggen R, Suchiman HED,

Lameijer E-W, Putter H, van den Akker EB, et al. 2013. Identification and systematic annotation of tissue-specific differentially methylated regions using the Illumina 450k array. *Epigenetics Chromatin* **6**: 26.

Slieker RC, Roost MS, van Iperen L, Suchiman HED, Tobi EW, Carlotti F, de Koning EJP, Slagboom PE, Heijmans BT, Chuva de Sousa Lopes SM. 2015. DNA Methylation Landscapes of Human Fetal Development. *PLoS Genet* **11**: e1005583.

Spiers H, Hannon E, Schalkwyk LC, Smith R, Wong CCY, O'Donovan MC, Bray NJ, Mill J. 2015. Methylomic trajectories across human fetal brain development. *Genome Res* **25**: 338–52.

Tserel L, Kolde R, Limbach M, Tretyakov K, Kasela S, Kisand K, Saare M, Vilo J, Metspalu A, Milani L, et al. 2015. Age-related profiling of DNA methylation in CD8+ T cells reveals changes in immune response and transcriptional regulator genes. *Sci Rep* **5**: 13107.

Urdinguio RG, Torró MI, Bayón GF, Álvarez-Pitti J, Fernández AF, Redon P, Fraga MF, Lurbe E. 2016. Longitudinal study of DNA methylation during the first 5 years of life. *J Transl Med* **14**: 160.

Weidner CI, Walenda T, Lin Q, Wölfler MM, Denecke B, Costa IG, Zenke M, Wagner W. 2013. Hematopoietic stem and progenitor cells acquire distinct DNA-hypermethylation during in vitro culture. *Sci Rep* **3**: 3372.